Exploring the Effect of Cathode Size on the Observable and Electrical Properties of Ball Plasmoid Discharges

By

Amber N Rose

Thesis

for the

Degree of Bachelor of Science

in

Chemistry

College of Liberal Arts and Sciences

University of Illinois

Urbana-Champaign, Illinois

2018

Table of Contents

1 Introduction

Ball plasmoids are a unique type of water-based plasma formed in air at atmospheric pressure. The term “plasmoid” is used to describe a plasma-magnetic entity that has a defined shape but no source of external power [1]. Generated by a discharge of stored energy from a capacitor bank, these plasmoids are uncharacteristically long-lived. For a plasma of this type, the expected recombination rates dictate that the plasmoid should dissipate in about a millisecond [2, 3]. However, these plasmoids are observed to last for several hundred milliseconds with no additional power input after the initial pulse.

The pulsed energy (on the order of tens of kJ) is released over the surface of grounded electrolyte. Energy as referred to here is defined as $U=\frac{1}{2}CV^2$, where U is the stored potential energy, V is the discharge potential, and C is the capacitance of the bank. Currents up to tens of Amps are achieved by charging the capacitor bank to several kiloVolts. As a result of this energy discharge, a jet is formed at the cathode, leading to the formation of a plasma. The ball rises due to buoyant forces, eventually detaching from the electrode and existing as an autonomous body for several tens of milliseconds. Although ball plasmoids have been produced and studied since 2002 [4], there is still much to be understood in regards to the underlying chemistry and physics, specifically relating to its stability and lifetime. Recently, we have presented detailed current and voltage profiles for two different electrode materials at a range of energies to more fully describe the electrical properties of ball plasmoid discharges [5]. In this work, we expand upon the characterization of the electrical properties of these discharges by changing the cathode size to gain a better understanding of how the diagnostic characteristics (observable, electrical, etc.) of the system responds to varied parameters. Although the physical characteristics (size, lifetime,

luminosity) of ball plasmoids have been briefly analyzed using a larger surface area electrode [6], the electrical diagnostics have not.

Due to several shared observable properties (luminous, spherical, sustained lifetime with no power source), ball plasmoids are considered to be analogous to the natural atmospheric phenomenon of ball lightning. Ball lightning has been reported for several centuries [7] and is usually associated with thunderstorm activity. Eyewitness accounts have reported luminous spheres dancing in the sky, lasting on the order of several seconds before vanishing silently or explosively [8]. One of the many complications in the attempt to study natural ball lightning is that it is exceedingly rare to witness: it is estimated that ball lightning is a one-in-a-million lightning event [9].

Although there have been many attempts to study this rare phenomenon, to date, there has been only one peer-reviewed observation of ball lightning, which occurred completely by accident. Cen et al. were observing natural cloud-to-ground lightning with slitless spectrographs when ball lightning occurred [10]. The analysis of their observations revealed a ball with a diameter of 1.1 m that had a luminous lifetime of 1.64 s. Additionally, they were able to capture an emission spectrum with strong continuous emission (400-700 nm) as well as silicon, iron and calcium emission lines. The detection of these emission lines is significant because these elements are known to be main components of soil, supporting theories that traditional ball lightning is a product of cloud to ground lightning striking soil [11]. As a result of the lightning strike to soil, the slow oxidation of and subsequent emission from metal nanoparticles is proposed as one mechanism for the slow energy release of ball lightning.

Due to the elusiveness of natural ball lightning and the similarities between ball lightning and laboratory ball plasmoids, these discharges serve as a unique system in which certain plasma

processes can be studied. Specifically, the anode in this system is a liquid electrolyte, making the system much more complex. In a traditional electrode system between metal plates, the anode cannot emit any positive ions and the current is only carried by the entering electrons from the cathode [12]. However, in the liquid electrolyte of this system, the water surface conducts differently (than a metal sheet, for example) and also could potentially introduce different charged species into the plasmoid (such as HCl from the electrolyte). Furthermore, gas phase water (neutral or ionized) has a tendency to cluster with other species which can collisionally quench the present excited species. Additionally, our electrode setup does not have an interelectrode gap as do others studying this same system [4, 11, 13-16], altering the properties of the circuit and therefore the plasmid itself. It has also been shown that anode-arc roots are developed during early stages of plasmoid formation and these arcs are highly dynamic as they interact with the liquid surface [13]. These arcs are interesting in this system because they occur on a time-scale faster than most high-speed videography can capture (with a lifetime no longer than 60 μs) but govern the earliest time period of plasmoid formation.

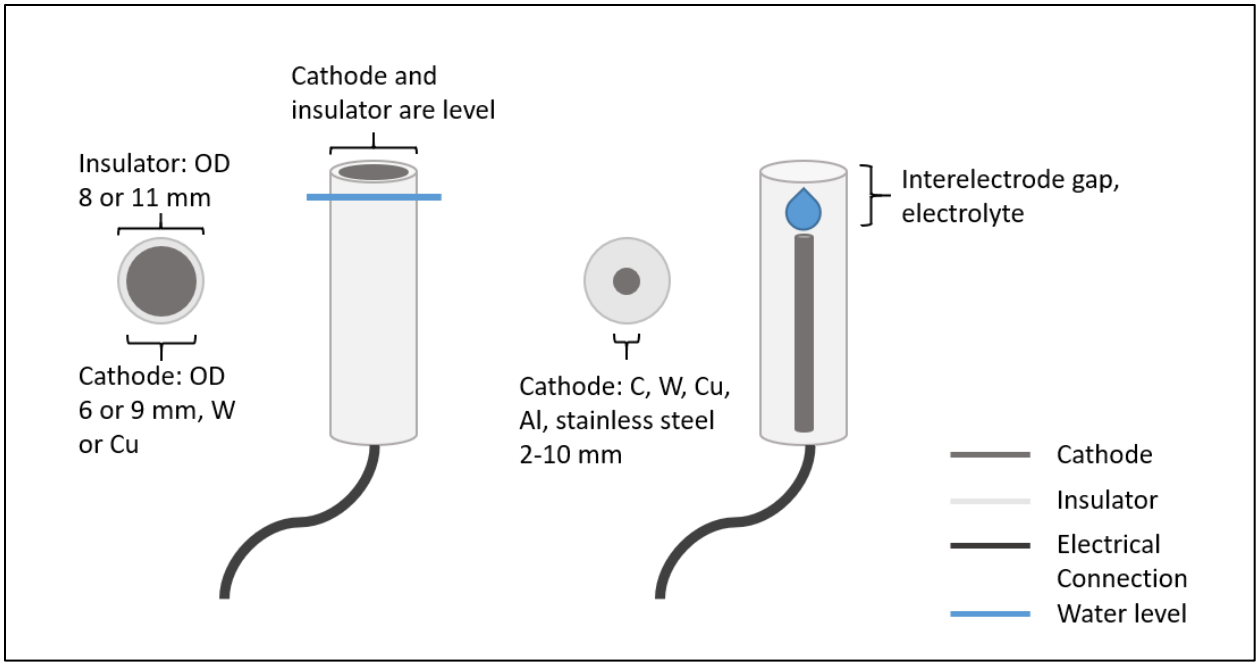

Figure 1. A simplified comparison of the electrode geometry used in this work (left) compared to an electrode geometry commonly used in other experiments (right).

This work is focused on the characterization of the electrical diagnostics (current and voltage) as well as the observable properties of the plasmoid itself (luminosity and lifetime) when the electrode geometry is altered from standard conditions. Although a wide range of cathode sizes (2-10 mm) and materials (C, W, Cu, Al, stainless steel) have been used in similar experiments [4, 6, 11, 13-16], there has been no comparison presented of diagnostics between two differently sized electrodes with all other components of the circuit remaining the same. Figure 1 shows a simplified schematic of the electrode geometry reported here compared to a typical geometry used in other experiments: a small diameter cathode with an air gap between it and the top of the insulator (usually with an inner diameter greater than the diameter of the cathode) filled with electrolyte. Increasing the size of the cathode increases the surface area of the cathode potentially altering how current and voltage dissipate through the system and into the plasmoid. As the surface area of the

cathode is increased (with the same input of energy), the current density is also decreased (Equation 1):

$$J = \frac{I}{A} \tag{1}$$

where J is the current density, I is the electric current, and A is the cross-sectional area of the conductor. A smaller current density through the cathode indicates a smaller power density (P_D=W/m^2) into the plasmoid, meaning that the electrical and observable properties of the plasmoid can be different. Although not explored in this work, a smaller power density could result in a decrease in the intensity of emission of excited species due molecules with less energy in the plasmoid. Additionally, a smaller current density could result in a smaller density of electrons with a sufficient energy to populate higher rotational and vibrational levels of excited species and therefore smaller rotational temperatures, assuming electron impact is one of the primary excitation mechanisms of this system. Future iterations of this experiment should include emission spectroscopy to more fully understand the effects of changing the cathode size on plasmoid composition.

2 Experimental

2.1 Plasmoid Generation

A ball plasmoid is formed by a pulse of stored energy from a capacitor bank over the surface of a grounded electrolyte (Figure 2). A Glassman EK series power supply is used to charge large parallel plate capacitors (873-1373 µF) to high voltages (typically 5000-8000 V). An Arduino Uno microcontroller is used to control the timing of three Ross Engineering E-series high voltage switches and a GigaVacG50WF vacuum relay. The Arduino microcontroller is also used to record the output for current (measured using a Hall-effect sensor) and voltage (measured using a voltage divider) measurements.

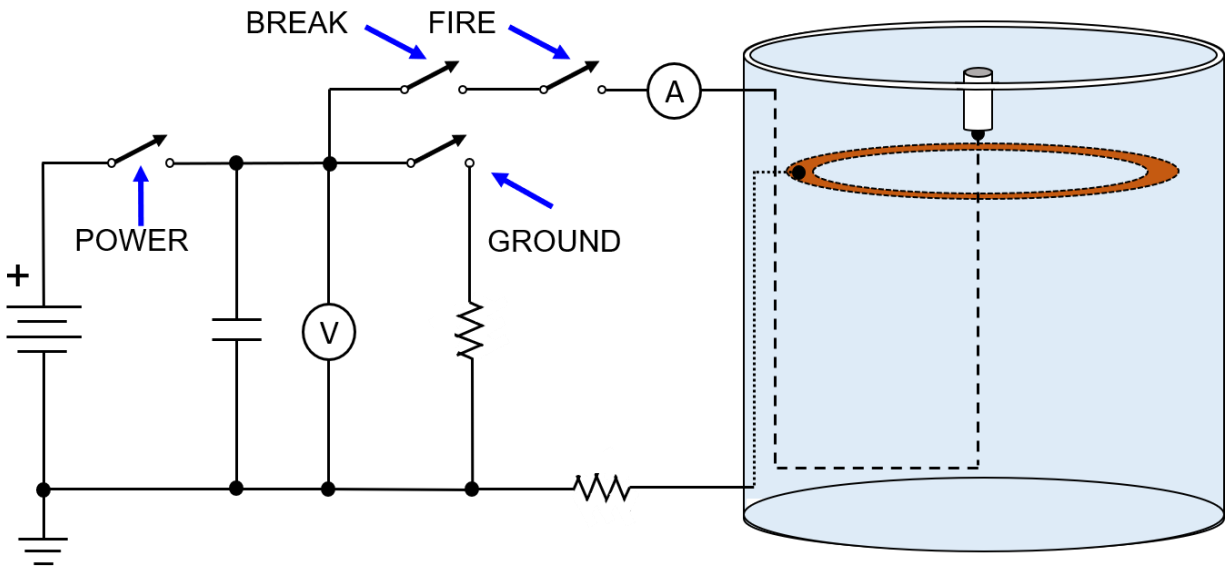

Figure 2. A simplified schematic of the discharge circuitry used to produce a ball plasmoid; Hall-effect sensor (A) and voltage divider (V). Figure adapted with permission from [5].

The energy in the charged capacitors is sent to an electrode that is partially submerged in a 20 L bucket of weakly conductive electrolyte. Conductivity of the electrolyte is set to

approximately 300 µS by adding concentrated HCl dropwise to deionized water. Conductivity is set to 300 µS in most cases because it has been shown to induce plasmoids with the longest lifetime [6]. All measurements reported herein are at 300 µS. The conductivity is measured using an Eutech Instruments Oakton PCSTest35 meter.

The cathode is typically a cylindrical tungsten rod (6 mm OD) insulated from the electrolyte by an alumina tube (6 mm ID, 8mm OD) (Figure 3). The cathode is set vertically such that the tip protrudes 1-2 mm above the surface of the electrolyte. In this custom electrode setup, the anode is a copper ring that is placed perpendicularly to the cathode and submerged several cm below the surface of the electrolyte (Figure 2). Tungsten is the cathode material most often used because of its robust nature, making it durable to the stress of discharges [6, 19]. However, a copper cathode is also substituted, with a quartz tube used as the insulator. The insulator serves to electrically isolate the cathode from the electrolyte so that the current travels above the surface of the water as opposed to through the water.

Figure 3. A close-up image of the cathode with an insulator that is flush to the tungsten rod (image was taken at an angle).

The plasmoids produced using this setup are approximately 20 cm in diameter at their full size and last for 200-400 milliseconds, under standard conditions. Figure 4 displays a series of images taken across the lifetime of a ball plasmoid discharge. It is also important to note that the size and lifetime of each ball plasmoid can vary from shot to shot. The stress of repeated discharges causes the surface of cathode and insulator to become jagged and uneven. This can alter the shape and symmetry of the plasmoid as it is produced. Additionally, changing various parameters (such as voltage, capacitance, cathode/insulator material and conductivity) can significantly alter the size, color and lifetime of the plasmoid. Data relating the changes in size and lifetime due to voltage and capacitance can be found in Section 3.

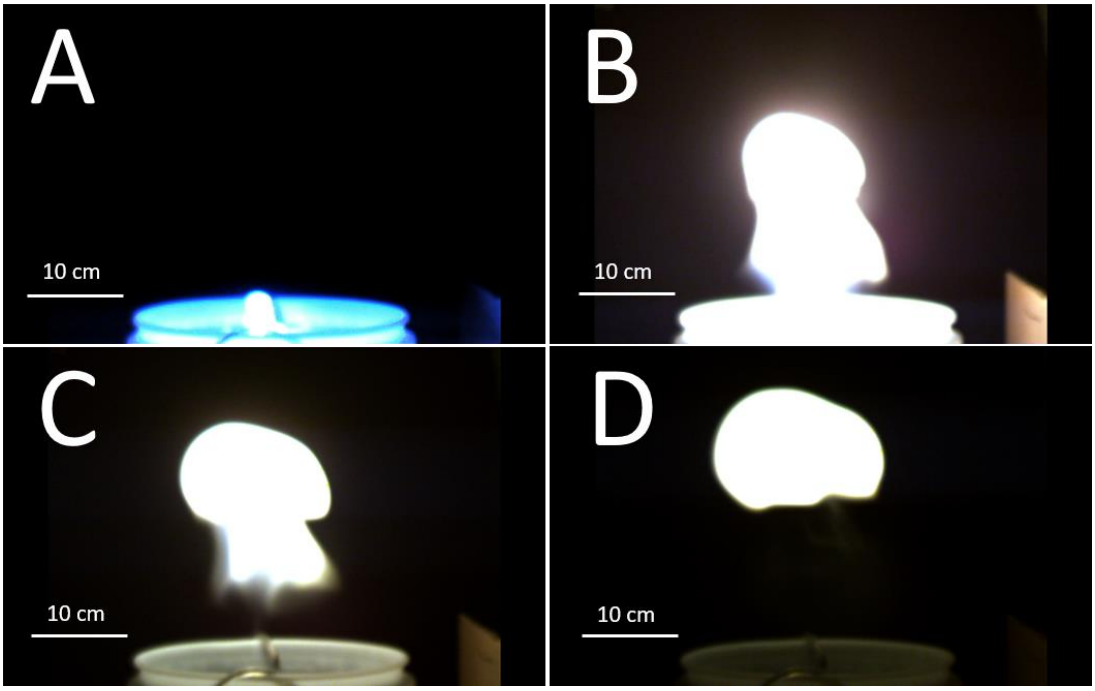

Figure 4. Images of a ball plasmoid discharge at various points in its lifetime taken by high-speed videography (tungsten, 8000 volts, 300 µS).

2.2 Videography

High-speed videography was performed as part of the diagnostics for each discharge to characterize various properties of the plasmoid. A PixelLink PL-B742U camera with a Computar LP390-30.5 lens was used. A series of color images were recorded with an exposure time of 1 ms and 85.3 frames per second. Using the frame rate, the visible lifetime of each ball plasmoid produced was determined by the number of frames for which the ball existed (from the first light at the cathode until no visual emission was observed). Likewise, the high-speed videos were used to produce a luminosity profile for each discharge using ImageJ.

2.3 Cathode Characteristics

The choice for cathode material and insulator has been extensively studied [6]. Tungsten and copper were chosen as the materials most frequently used due to the highly conductive nature of these materials (current maxima can exceed 100 amps) as well as their robust nature. A material that can withstand the high temperatures and frequent repeated discharges is needed in order to prevent considerable breakdown and the need to polish the surface often. These two cathode materials (and corresponding insulators) produce plasmoids with similar shape, lifetime, and current maxima (Figure 5). The plasmoids produced with these different materials do differ, however, in size, luminosity and color. Figure 6 shows that while both plasmoids have a similar shape, copper is smaller and less luminous with a blue hue (as a result of emission from excited states of neutral copper). Furthermore, the cathode material does not significantly alter the maximum current of the discharge, thus suggesting that the cathode material does not have considerable impact on the electrical characteristics of the discharge.

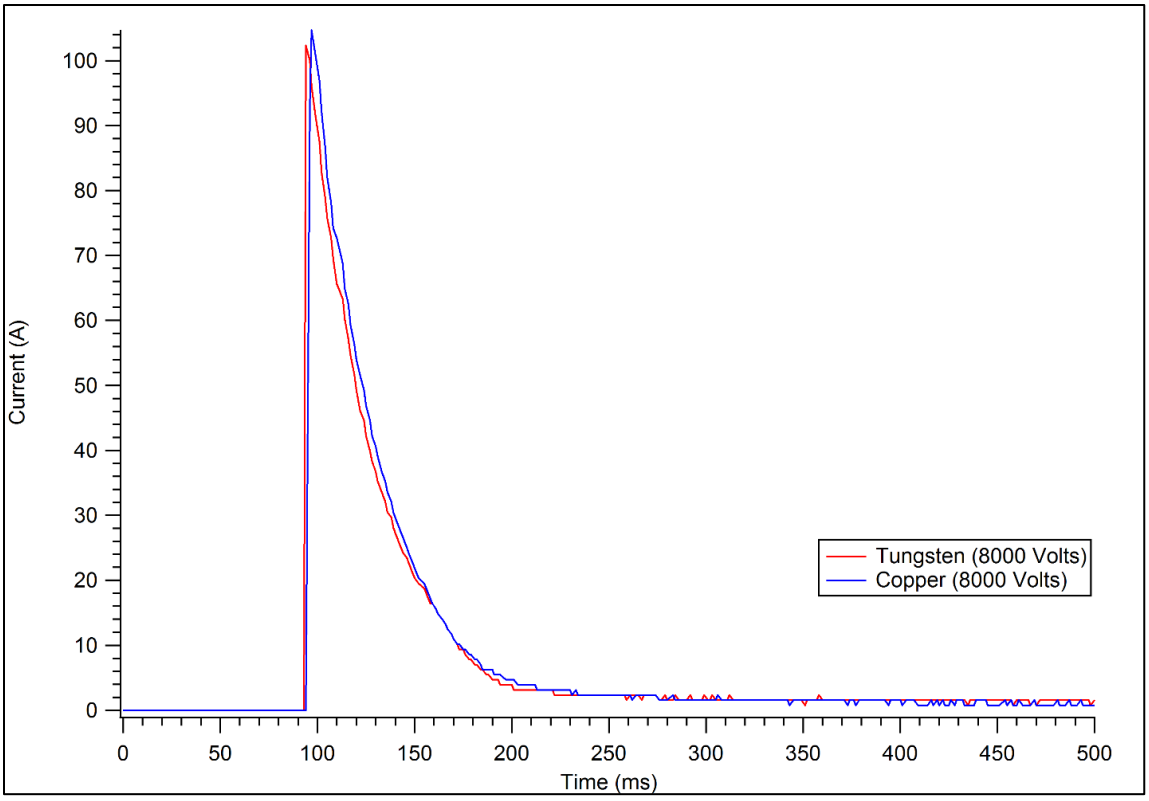

Figure 5. A comparison of current traces over the lifetime of a ball plasmoid discharge for the two materials used most frequently. Both traces were obtained at identical conditions (8000 Volts, 300 µS, 873 µF) on the same day.

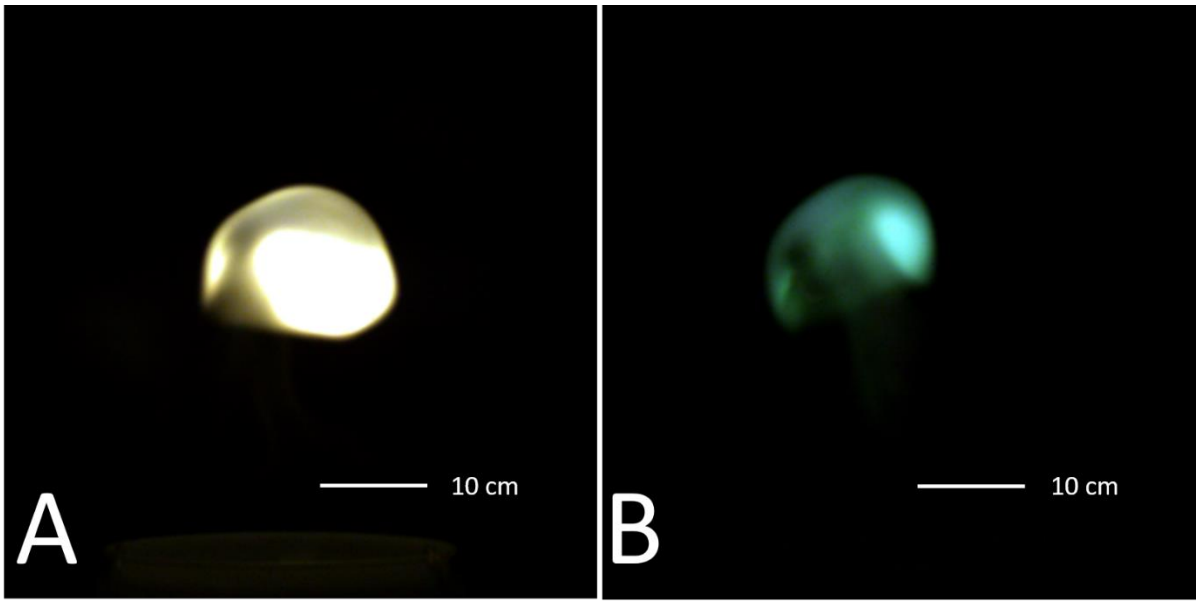

Figure 6. Images of autonomous ball plasmoids at approximately the same point in the lifetime ([A] tungsten, [B] copper).

The standard copper electrode used has a diameter of 6 mm and a surface area 28.27 mm^2. To study how the diagnostic characteristics of the plasmoid (current, voltage, luminosity, and lifetime) change as a function of cathode size, the diameter of the electrode was increased to 9 mm with a surface area of 63.62 mm^2, more than doubling the surface area. Additionally, two capacitances were used (873 and 1373 μF) to increase the energy available to exploit potential differences in the diagnostic parameters for each discharge as the surface area of the cathode was increased. All data presented in Section 3 were taken using a copper electrode.

3 Results and Discussion

3.1 Phases

The formation of a ball plasmoid has been categorized by Stephan et al. into three sequential stages (Figure 7): pre-initiation, build-up, and detachment [14]. The pre-initiation phase begins when the switch to the electrode that controls the flow of current closes (at 50 ms), sending the built-up energy through the circuit and to the cathode. In this phase, a plasma does not form. The build-up phase is marked by the formation of a cathode spot once the current density is sufficient to begin plasma formation. The current flows much more freely and increases rapidly (starting at ~100 ms). The plasma continues to grow at the cathode tip, becoming large enough that contact between the plasma and the electrolyte is produced, with streamers extending across the surface of the electrolyte. As the plasma continues to grow, it also begins to rise due to buoyant forces. Cooler, room temperature air, surrounds the plasma, separating it from the surface of the electrolyte, decreasing the surface area across which contact can be made. The detachment phase begins when the current reaches its maximum and the formed ball is no longer connected to the cathode tip. During this phase, the ball is observed to last autonomously up to 100 milliseconds before dissipating. The lifetime of these plasmoids from the beginning of plasma formation to the dissipation of the autonomous body ranges from 200-400 ms, depending on the voltage and capacitance used for the discharge.

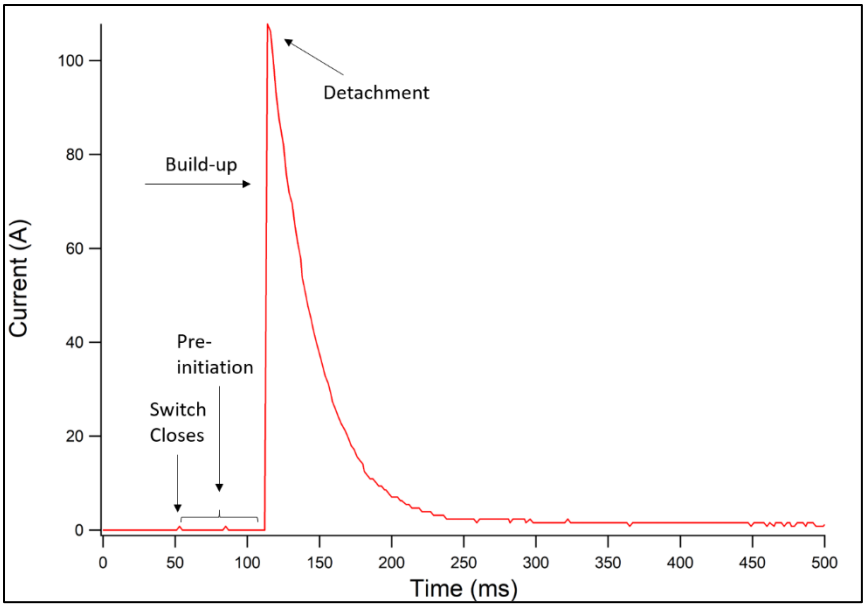

Figure 7. An example current trace of a ball plasmoid discharge with the three phases of development labelled (copper, 8000 volts, 300 µS).

However, Stelmashuk and Hoffer assert that previous images of plasmoid phases are too overexposed to be useful in detailed analysis [13]. The over-exposure obscures some of the highly complex physical processes that occur during formation (while some processes may even be occurring on a time scale faster than can be imaged). By performing high-speed videography with a 47 µs exposure time, they concluded that plasmoid generation can be classified by four distinct phases: initiation, breakdown and explosion, buildup, and an autonomous phase. Additionally, the electrode geometry is altered in one key way that is different than described above. In this configuration, the insulator is filled with a conducting solution, surrounding the cathode.

The initiation phase begins with a triggering signal and the high-voltage relay makes a connection. The capacitor bank begins to discharge through the system and sparks can be seen, electrically connecting the electrolyte surface with the liquid surface of the cathode and lasting for no more than 60 µs. The breakdown and explosion phase occurs when all but one of the sparks

disappear and electrical breakdown occurs followed by a water explosion. At this moment, the current rapidly increases to its peak value. The current is then redirected to the last spark, creating an arc transition that is eventually absorbed in the weakly ionized plasma, water vapor and bubbles. The buildup phase is marked by the appearance of a jet emitting a plasma along its vertical axis. The jet is electrically connected to the surface of the electrolyte by the arcs from the explosion phase (these have been previously identified as streamers [13]). As the plasmoid rises, these arcs lengthen, their conductivity is lost and the electrical current flowing through them is decreased. When the jet disappears, the autonomous phase begins and is characterized by a current drop to 0 A.

Due to the nature of the electrode geometry used in these experiments and the limitation to our videography, there does not seem to be a quantitative way for determining these phases, most notably the autonomous phase. The interference of water from the electrolyte complicates the electrical profiles that can be obtained. The presence of two time constants (see Section 3.6) also complicates the situation since there is always a small electrical connection due to the spark channels. Therefore, we cannot determine the point in time that the ball detaches from the electrode from electrical profiles or video. This work does not serve to support one argument of the different phases of plasmoid formation but rather to present two competing theories of a critical aspect in the understanding of ball plasmoids.

3.2 Luminosity

Figure 8 shows an example set of overlaid luminosity profiles for plasmoid discharges from 5-8 kV. Profiles were acquired using the PixelLink camera (as described above) and processed using ImageJ. The maximum and integrated intensities have arbitrary units because ImageJ provides brightness relative to the background of the image. The integrated intensity values are

averaged over three trials at each voltage. The time axis in Figure 8 was scaled to accommodate different numbers of image frames for each profile and the number of frames was then converted into a time scale.

Table 1 summarizes the integrated intensity values for each set of conditions. It is evident from these values and the luminosity profiles that the maximum luminosity of the discharges increases with voltage. This trend holds for both capacitances and cathode diameters. The overlaid luminosity profiles are staggered as a result of each plasmoid being unique and the frame with maximum brightness is different, although generally at the same point in time. Likewise, the error associated with the integrated intensities is large and varies from shot to shot for the same reason.

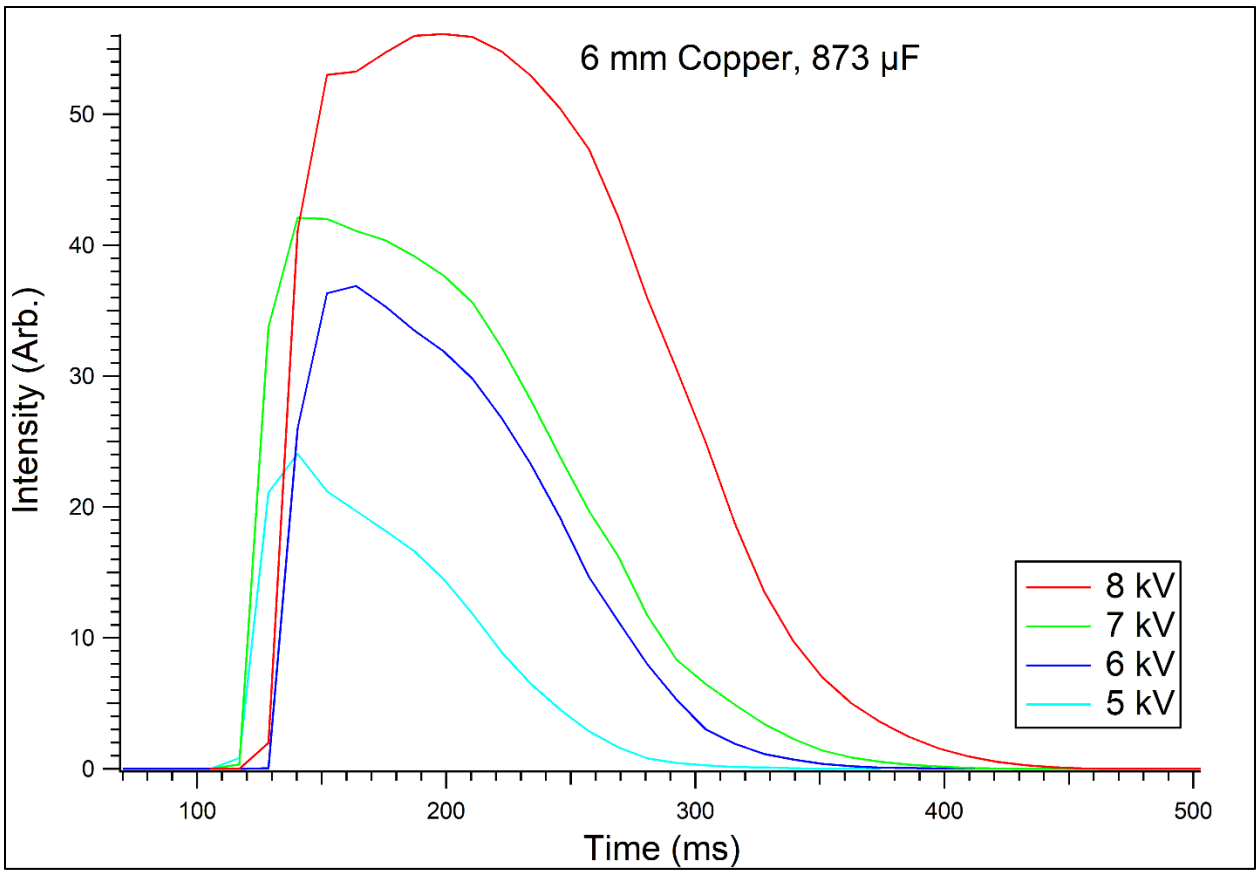

Figure 8. An example plot relating the luminosity profiles over the course of ball plasmoid discharges.

Table 1. Integrated intensity of ball plasmoids' luminosity over the entire lifetime as a function of the discharge voltage, capacitance and cathode size.

	Integrated Intensity (Arb.)			
Voltage (kV)	**6 mm, 873 µF**	**6 mm, 1373 µF**	**9 mm, 873 µF**	**9 mm, 1373 µF**
5	192 ± 42	426 ± 153	135 ± 40	230 ± 50
6	374 ± 41	532 ± 114	328 ± 19	480 ± 38
7	430 ± 38	697 ± 137	457 ± 62	635 ± 81
8	733 ± 51	920 ± 74	494 ± 44	751 ± 77

The integrated intensities summarized in Table 1 indicate that, at the same cathode diameter, the luminosity of the plasmoids increases as the capacitance of the system increases. As more energy is put into the plasmoid, by increasing the starting discharge potential and the capacitance, the greater the luminosity will be. More energy put into the plasmoid increases the number of excited species that can emit radiation and thus increasing the luminosity. When increasing the diameter of the cathode, no additional energy was put into the system, therefore it can be proposed that the luminosity over the course of the plasmoid's lifetime should not change significantly. Additionally, since these luminosity measurements are integrated over the entire lifetime, it cannot be suggested that the shape of the luminosity profiles are different (i.e. brighter for a shorter period of time) as a result of a change in current flow from the larger electrode. While some of the luminosity values for the large cathode appear to be of similar magnitude to the smaller cathode counterparts, others (such as at 8 kV) are smaller. This disparity can be explained by the current maxima for these conditions (see section 3.4). The current maxima for the larger cathode are smaller for every set of conditions. With less power being put into the plasmoid, the population of excited species will be lower and the luminosity will be reduced, as seen by luminosities at lower discharge potentials.

3.3 Lifetime

The lifetime of ball plasmoid discharges is one of the most unique and fascinating aspects. The lifetime of each plasmoid is determined by the high-speed videography from each trial: for each video, the number of frames is counted from the first light at the cathode tip until the autonomous body has fully recombined and no visual emission is observed. Using the number of frames of visible emission and the frame rate of the camera (85.3 fps), the lifetime is easily determined. For plasmoids at 5-8 kV and with a capacitance of 873-1373 μF, the lifetime of each ball is normally between 200-400 ms.

Table 2. The averaged lifetimes of ball plasmoid discharges as a function of the discharge voltage, capacitance and cathode size.

	Lifetime (ms)			
Voltage (kV)	**6 mm, 873 μF**	**6 mm, 1373 μF**	**9 mm, 873 μF**	**9 mm, 1373 μF**
5	218 ± 39	293 ± 62	195 ± 27	226 ± 34
6	264 ± 29	316 ± 62	250 ± 28	301 ± 39
7	301 ± 34	391 ± 69	301 ± 45	348 ± 58
8	352 ± 33	402 ± 45	348 ± 57	379 ± 35

Table 2 summarizes the average lifetime of ball plasmoids for the voltage, capacitance and cathode size range explored in this work. For each reported lifetime, three trials were averaged. Similar to that of the luminosity, the lifetime of ball plasmoid discharges increases as the voltage and capacitance increases. As the cathode size was increased, the same trends are observed. However, at the same conditions (voltage and capacitance), there is little change in plasmoid lifetime attributed to increasing the surface area. It has been shown in [20] that as the voltage is increased, the lifetime of the plasmoid also increases but the relationship is not linear: a maximum lifetime does occur within the conditions tested. Figure 9 also supports that there are some

saturation effects noticeable as the voltage is increased. However, to fully support this assertion, data need to be collected over a broader range of discharge voltages.

Again, no additional energy was put into the plasmoids when the cathode size was increased. This observation suggests that since there is little change to plasmoid lifetime due to the surface area of the cathode, it is most likely the energy that determines how long the ball persists, within this range of conditions. The slight decrease in plasmoid lifetime for the larger cathode can also be a result of the decreased current, but it appears that this current decrease does not make as large of an impact on the lifetime as it does on the luminosity.

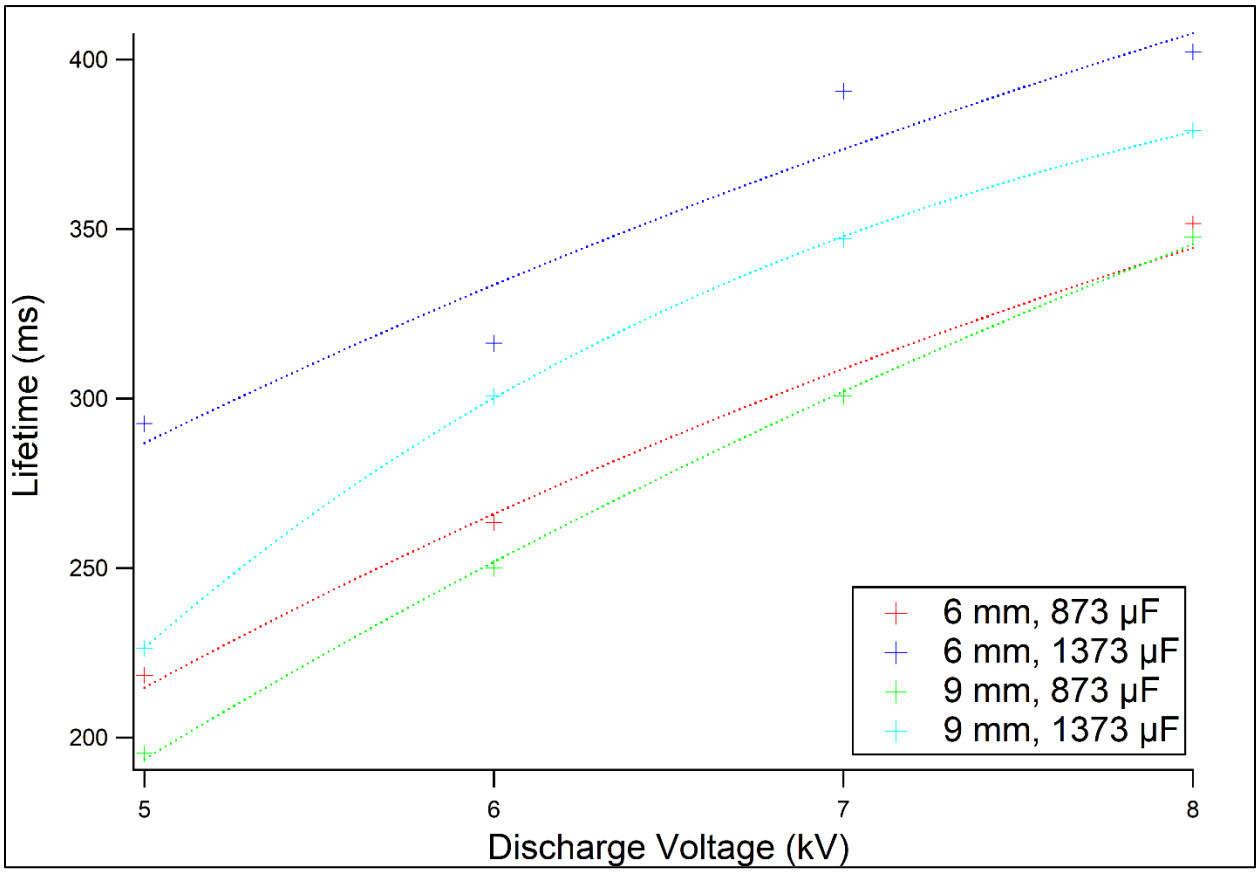

Figure 9. A comparison of the lifetimes of ball plasmoid discharges as a function of the discharge voltage with an exponential fit applied.

There is a significant error in the averaged measurements due to the inherent shot-to-shot differences between each discharge (~3-15%). Additionally, the lifetime determination is limited by the fact that there is 11.7 ms between each successive frame. Although the frame rate set for the camera is 85.3 fps, the limitation is the exposure time permitted (1 ms). Therefore, although for each frame of 11.7 ms, only 1 ms of light is captured. Because lifetime was determined by counting from the first frame where visible emission was observed, it is possible that visible emission was observable up to 10.7 ms earlier, but not detected by the camera. This possibility is also present for the end of the plasmoid's lifetime, allowing for a combined 21.4 ms of error in the lifetime of each plasmoid in addition to the shot-to-shot differences in lifetime.

3.4 Current

As the discharge potential of ball plasmoid discharges is increased, the current that flows through the system into the plasmoids also increases. Figure 10 displays an example set of current traces over 600 ms as the discharge potential is increased from 5 to 8 kV. As the discharge potential is increased, the maximum current also increases linearly (Figure 11). Table 3 also clearly supports this trend for all conditions. At the 6 mm cathode size, the maximum current is the same (within experimental error) for increased capacitance at 5 and 6 kV. However, at 7 and 8 kV, the maximum current increases by several amps as the capacitance is increased. In contrast, at the 9 mm cathode size, there is very little change in maximum current as the capacitance is increased.

It is an interesting observation that the maximum currents for the larger cathode do not achieve the same levels as do those for the smaller cathode. A possible explanation for this feature is that when acquiring the data for the small cathode, discharges were taken at various points during the day and across more than one day. Whereas data for the large cathode were taken on the same

day within a much narrower window of time. Repeated discharges increase the temperature of the electrolyte by several degrees, especially at the higher voltages and capacitance. As the temperature of the water increases, the resistance of the water also increases, which in turn prevents the current from flowing as freely.

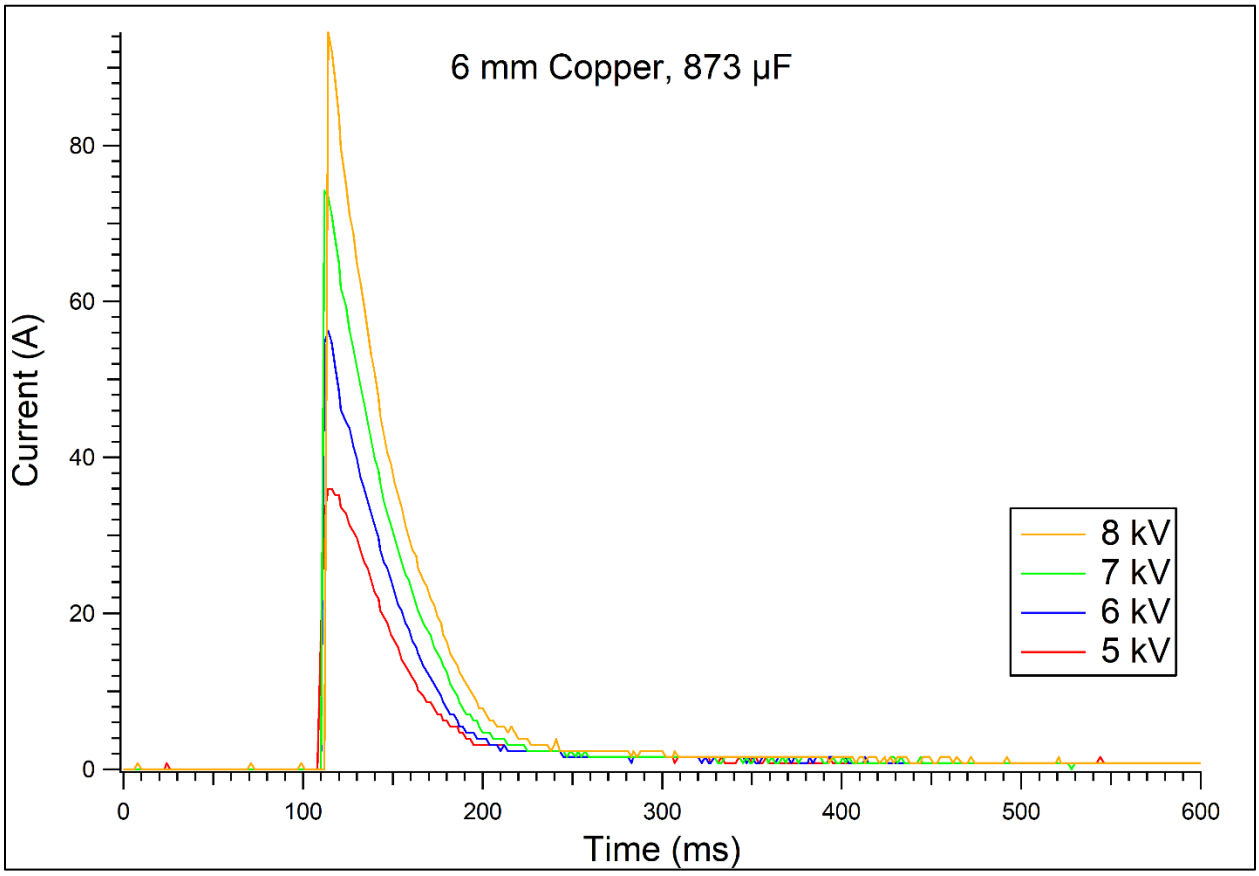

Figure 10. An example plot comparing the current traces over the course of ball plasmoid discharges.

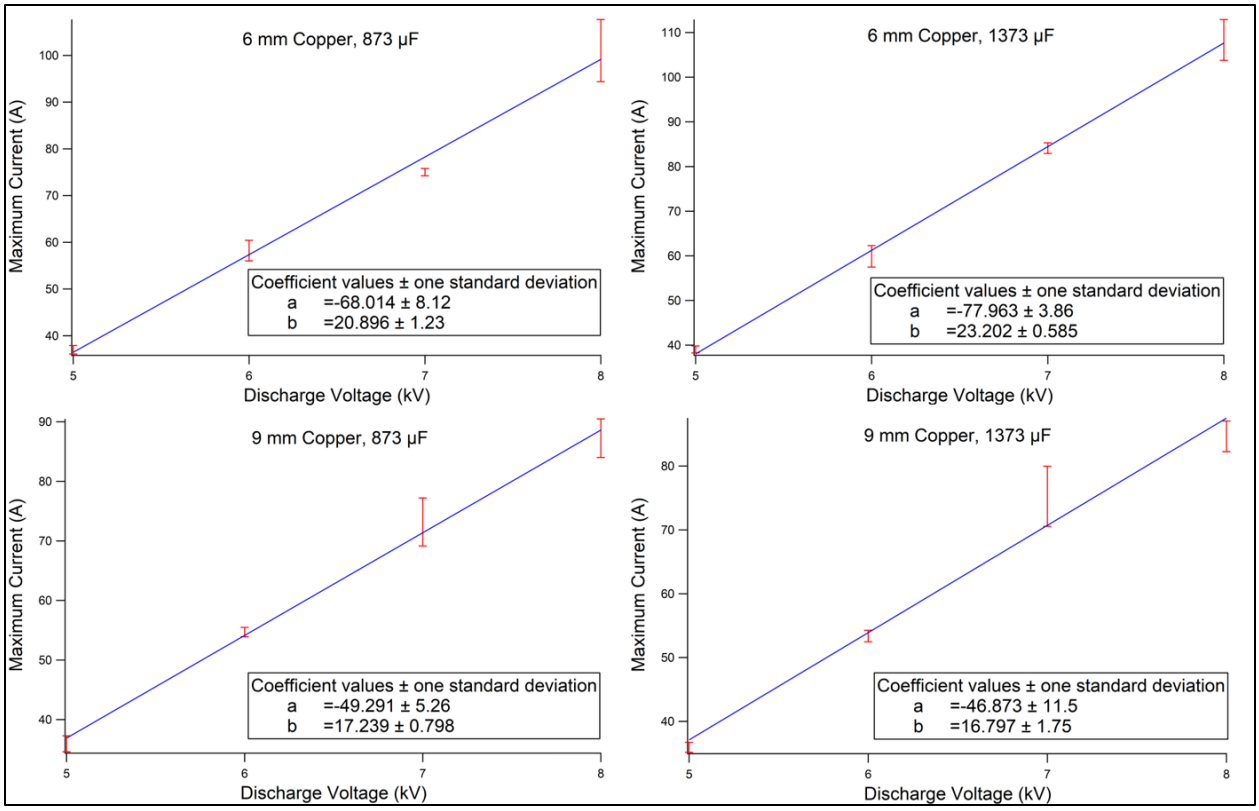

Figure 11. An array of plots of the averaged maximum currents at the various discharge voltages for the different capacitances and cathode size.

Table 3. The maximum current values obtained from the current trace obtained for each discharge. Each current value is the maximum current averaged across three trials.

	Maximum Current (A)			
Voltage (kV)	**6 mm, 873 µF**	**6 mm, 1373 µF**	**9 mm, 873 µF**	**9 mm, 1373 µF**
5	37 ± 0.9	39 ± 0.8	36 ± 1.4	36 ± 0.8
6	58 ± 2.2	60 ± 2.4	55 ± 0.8	53 ± 0.9
7	75 ± 0.8	84 ± 1.2	73 ± 4.0	75 ± 4.7
8	101 ± 6.6	108 ± 4.6	87 ± 3.3	85 ± 2.4

Since the cross-sectional area of the cathode changes, the current density also changes. Table 4 summarizes the current densities from the maximum current at each condition and the corresponding surface area of the cathode used. As expected, as the size of the cathode is increased, the current density decreases by ~ 40% in all cases.

Table 4. Current densities calculated from the maximum current and surface area of the cathode.

	Current Density (A/mm^2)			
Voltage (kV)	**6 mm, 873 µF**	**6 mm, 1373 µF**	**9 mm, 873 µF**	**9 mm, 1373 µF**
5	1.3 ± 0.03	1.4 ± 0.03	0.57 ± 0.02	0.57 ± 0.01
6	2.1 ± 0.08	2.1 ± 0.08	0.86 ± 0.01	0.83 ± 0.01
7	2.7 ± 0.03	3.0 ± 0.04	1.2 ± 0.06	1.2 ± 0.07
8	3.6 ± 0.23	3.8 ± 0.16	1.4 ± 0.05	1.3 ± 0.04

Another unique feature regarding current flow is how the current travels from the cathode to the electrolyte. Figure 12 compares the tip of each cathode after many discharges. Both copper cathode and quartz insulator show signs of distress (black charred spots, green oxidation deposits, and melted copper/quartz in the small gap between the insulator). However, there are also distinct marks where the current travels out of the system. Upon closer inspection, these marks are contained to the outer edge of both cathode rods and there are a similar number of these marks on each cathode. These marks suggest that current does not flow from the entirety of the available surface area of the cathode, but rather through the shortest path to form arc channels with the grounded electrolyte. When the cathode was set below the level of the insulator, however, these marks were no longer concentrated along the edge of the rod but contained to the center. This observation indicates that the depth of the air gap alters the path that the current takes to ground: the current searches for the path of least resistance to the electrolyte and that path is found more easily through the center of the cathode rather than at the edges.

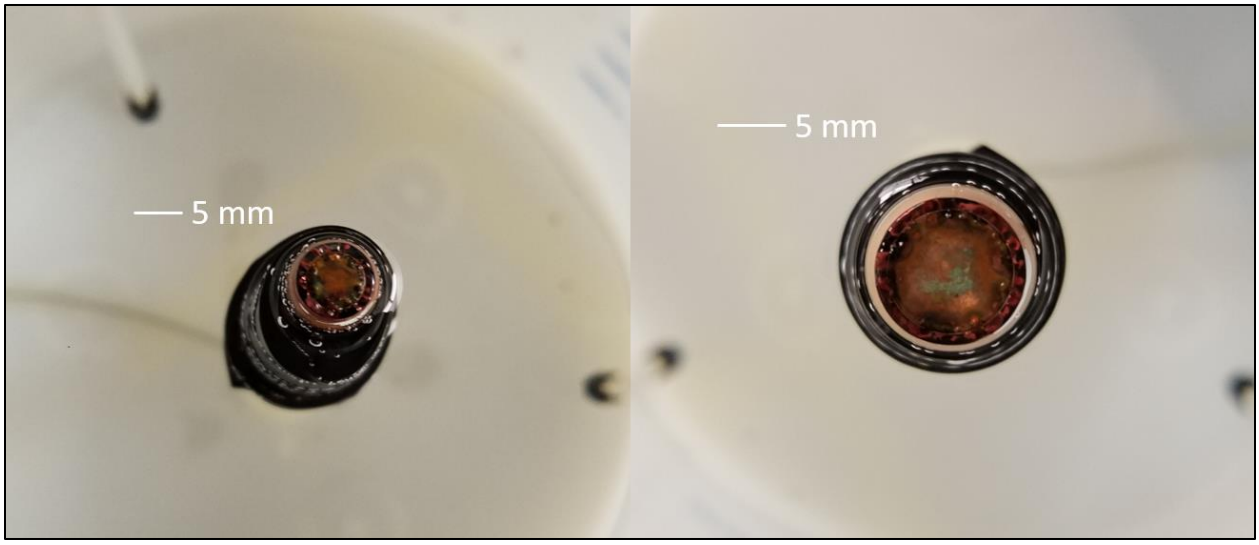

Figure 12. A comparison of each cathode after a full set of discharges. [Left: 6 mm, Right: 9 mm]

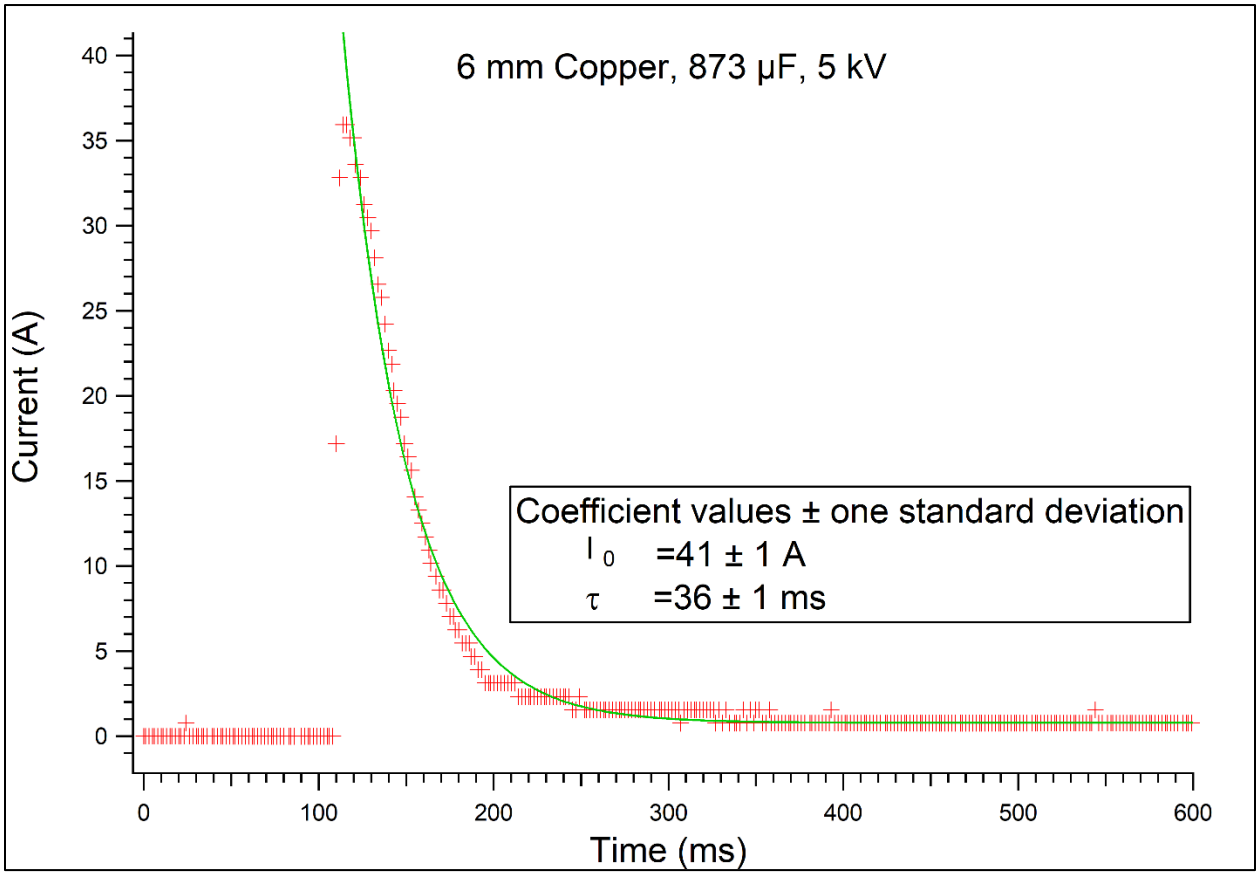

Figure 13. An example fit (green) to a current profile (red). The current is fit to a single exponential.

Figure 13 shows an example analysis of the current characteristics of ball plasmoid discharges (voltage will be discussed separately). The current profile was fit to an exponential (starting from the peak current at ~115 ms until the switch closes at ~600 ms) with the form of Equation 2:

$$y = I_0 + Iexp\left\{\frac{-(t - t_0)}{\tau}\right\} \quad (2)$$

where I_0 represents the remaining current in the system, I represents the amplitude of the exponential decay (the starting current), $t\text{-}t_0$ is the horizontal offset of the fit (the fit only applies to the decreasing portion of the current profile), and τ is the time constant, defined by Equation 3:

$$\tau = RC \quad (3)$$

where R is the resistance of the circuit (Ohms), and C is the capacitance (Farads). I_0 is consistent for each current fit for each cathode size and capacitance and is considered 0 A. The amplitude I increases as the voltage increases.

The time constants summarized in Table 5 are averaged values over all discharge potentials for each condition of cathode size and capacitance. If the resistance of the system is considered to be unchanged between each trial, it can be concluded that the time constant is primarily governed by the capacitance of the system. This is supported by the time constants calculated from the current profiles: at each cathode diameter, the time constant increased slightly as the capacitance increased. As the capacitance is increased by 57%, the time constants increase by 37% (for 6 mm) and 50% (for 9mm). Since the time constant appears to be strongly influenced by capacitance, it does not seem that the cathode size plays a significant role in how the current is dissipated through the system. The data in Table 4 confirm that within the experimental error, there is little change to the time constants as the diameter of the cathode is increased.

Table 5. Time constant values determined by an exponential fit to the current profiles. Each value is an average of 12 trials for a given cathode size and capacitance.

	6 mm, 873 µF	**6 mm, 1373 µF**	**9 mm, 873 µF**	**9 mm, 1373 µF**
τ (ms)	35 ± 2	48 ± 3	36 ± 1	54 ± 3

3.5 Resistance

The resistance of the system (the physical components of the circuit separate from the plasmoid) could be calculated in two ways from the experimental data obtained from the current profiles (summarized in Table 6). The first is by using Ohm's Law (V=IR) and the slope of the line of the plots of peak current vs discharge voltage (Figure 11). The second is by using the time constant values (Table 5) obtained from the exponential fits and Equation 2. Although both methods produce similar values of resistance, due to the nature of the method, using τ to calculate these values seems to be more accurate. This is because τ is a result of a fit to the entire current profile rather just the peak current. Additionally, it is not expected that the increase in cathode size should make a drastic change to the overall resistance. Using the definition of resistance (Equation 4), the resistance for the 6 mm cathode is 2.97×10^{-3} Ω and the resistance for the 9 mm cathode is 1.32×10^{-4} Ω. In our circuit, there are two main ballast resistors of 1.7 kΩ and 50 mΩ. Such small resistances from the cathode itself have negligible impact to the total resistance of the entire system.

$$R = \frac{\rho L}{A} \tag{4}$$

ρ is the resistivity of copper (1.68×10^{-6} ohm•m), L is the length of the conductor (5 cm), and A is the cross-sectional area of the conductor (28.27 mm^2 and 63.62 mm^2).

Table 6. A summary of the resistances calculated for this system by two methods.

	6 mm, 873 µF	**6 mm, 1373 µF**	**9 mm, 873 µF**	**9 mm, 1373 µF**
R [τ] (Ω)	48 ± 3	43 ± 1	58 ± 3	60 ± 6
R [Ohm's law] (Ω)	40 ± 2	35 ± 2	41 ± 1	39 ± 2

3.6 Voltage

Unlike current, the voltage is set at the beginning of the discharge and decreases monotonically, whereas current increases rapidly before reaching a maximum. The peak current is achieved only a few milliseconds after the voltage begins to decrease (Figure 14). Additionally, the voltage profile is governed by a biexponential with the form of Equation 5. The significance of this observation is discussed extensively in [5] and below. An example analysis is shown in Figure 15. The biexponential fit begins when the voltage of the system begins to decrease and ends when the switch closes at 600 ms.

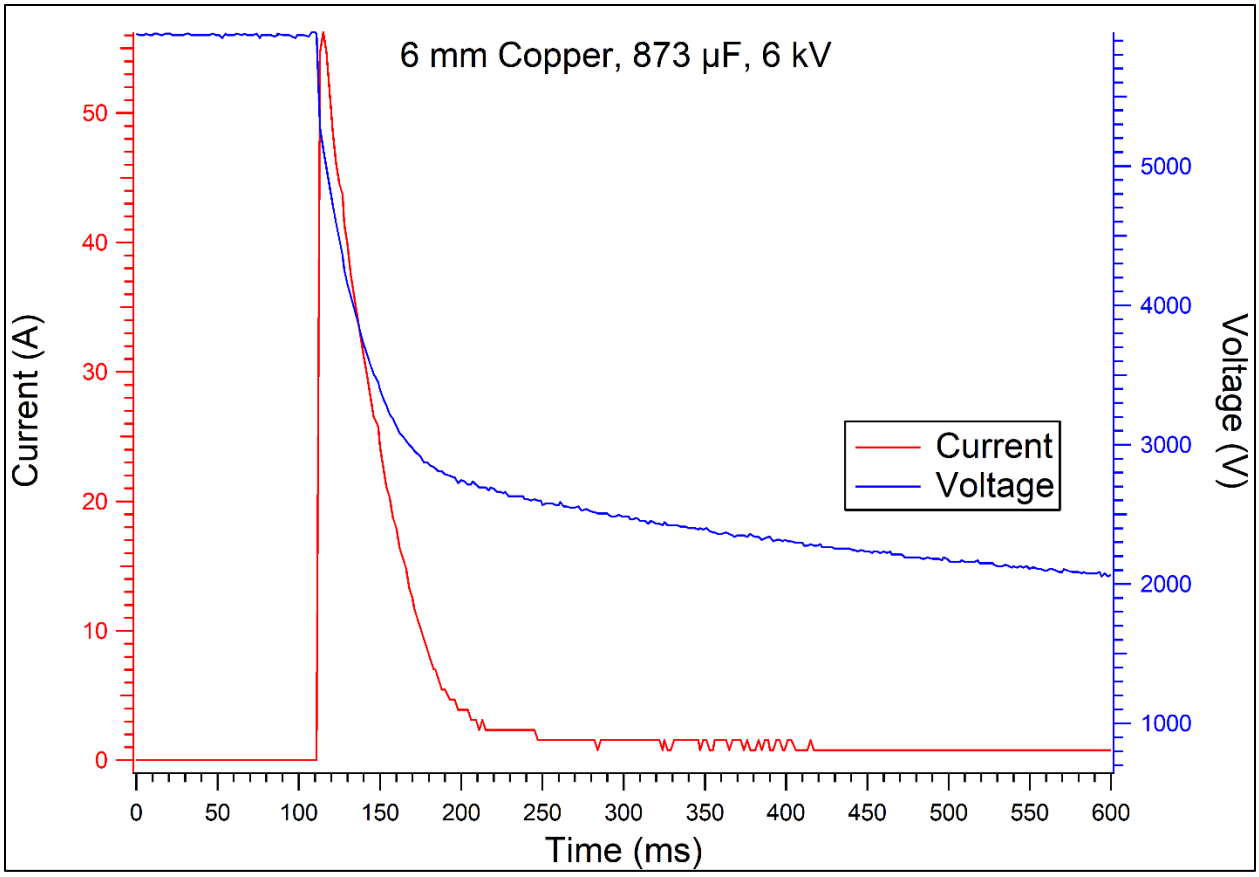

Figure 14. An example comparison of the current and voltage profiles obtained from a ball plasmoid discharge.

$$y = V_0 + V_1 exp\left\{\frac{-(t - t_0)}{\tau_1}\right\} + V_2 exp\left\{\frac{-(t - t_0)}{\tau_2}\right\} \quad (5)$$

In the biexponential equation, V_0 represents the remaining potential across the capacitor once the current flow to the cathode has been halted by the closing of the fire switch at 600 ms and ranges from 1800-2200 V. The capacitor bank for the discharges in our laboratory is never fully discharged after the 600 ms used for analysis. V_1 and V_2 are the amplitudes of the respective time constants (Volts). The value of these amplitudes increases as the discharge potential increases from 5-8 kV and $V_0 + V_1 + V_2$ is equal to the starting voltage. The time constants, τ_1 and τ_2, are summarized in Table 7.

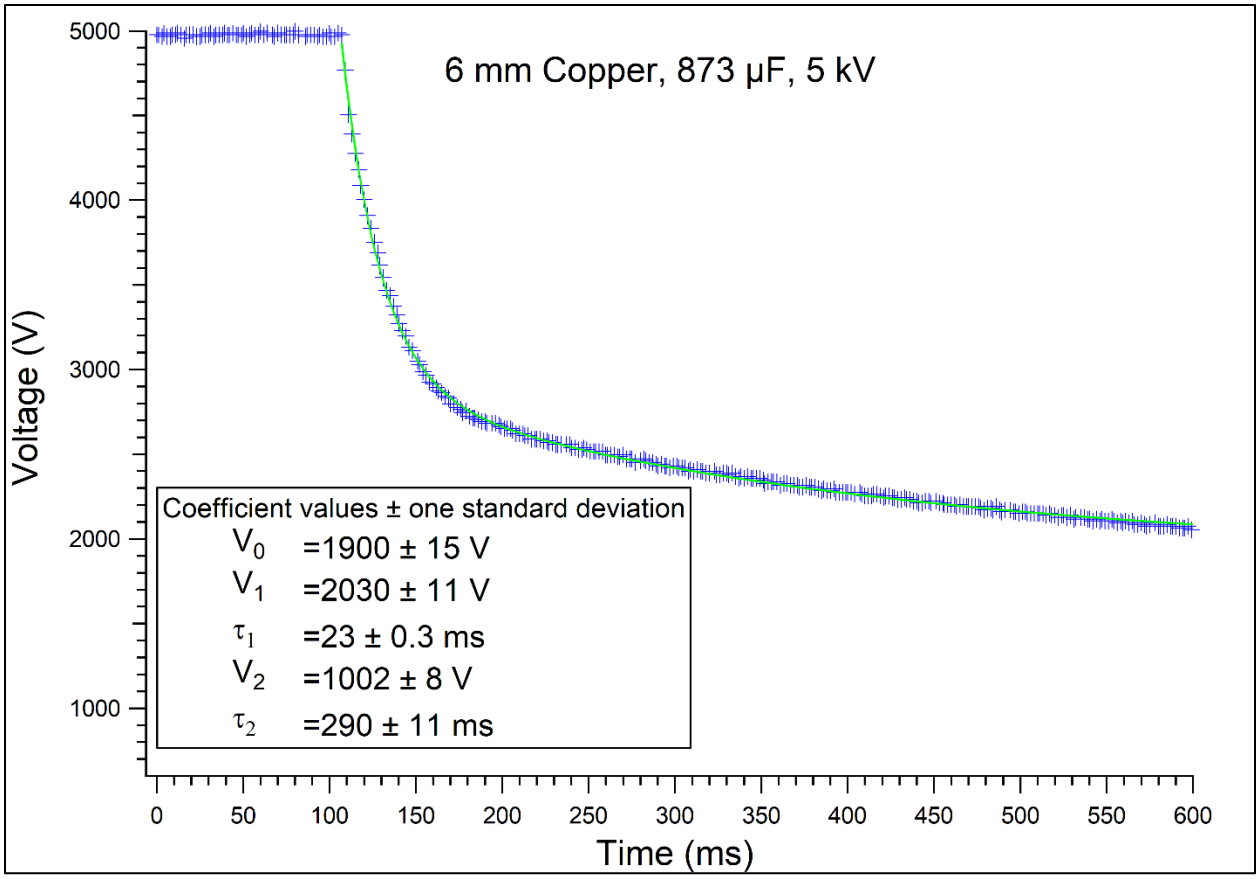

Figure 15. An example fit (green) to a voltage profile (blue). The voltage is fit to a biexponential (Equation 5).

Table 7. Time constant values determined by a biexponential fit to the voltage profiles. Each value is an average of 12 trials for a given cathode size and capacitance (three trials for each voltage).

	6 mm, 873 µF	**6 mm, 1373 µF**	**9 mm, 873 µF**	**9 mm, 1373 µF**
τ_1 (ms)	25 ± 2.1	35 ± 4.0	26 ± 2.3	36 ± 5.6
τ_2 (ms)	280 ± 25.8	350 ± 47.4	243 ± 26.1	255 ± 54.6

Results from the biexponential fit indicate that, at 6 mm and 873 µF for example, a fast time constant τ_1=25 ± 2.1 ms governs the earliest stages of ball plasmoid formation and a larger constant τ_2=280 ± 25.8 ms governs the later stages. The presence of two time constants is significant due to the electrode geometry used [5]. τ_1 is the faster of the two constants by an order of magnitude, meaning that during the beginning of the discharge, there is a significant amount of

current flow and a dramatic decrease in voltage. During the time that τ_1 is dominant, a jet (as mentioned in [13]) is produced at the tip of the cathode. While there are two time constants, τ_2 is not a distinct phase, but rather, is always present and only dominant at later times when most of the current has already dissipated through the system. The jet formed previously is no longer present but there is still an electrical connection through the spark channels due to the proximity of electrolyte to the cathode. In [5], we have indeed shown that by altering the geometry of our electrode such that the cathode tip is well below the surface of the insulating tube, therefore increasing the air gap between the electrolyte and the cathode, changing the path of the current as it travels to the electrolyte. At this condition, the voltage waveform is then governed by a single exponential. The single exponential is observed when only spark channels are formed, but no jet. It is also an interesting point that when the cathode was set below the level of the insulating tube, the spots on the cathode were no longer set along the edge of the rod, but rather, located at the center of the tip of the cathode. Again, this means that the easiest path to ground is now through the center of the cathode tip, rather than the edges.

Additionally, as the capacitance is increased (for each cathode size), both τ_1 and τ_2 become larger. Comparing the time constants at the same capacitance, there is not much of an effect on τ_1 when the cathode size increases. However, there seems to be a decrease in the magnitude of τ_2. τ_2 at 873 μF is only slightly faster than the corresponding constant at 6 mm. At 1373 μF, the time constant is significantly faster than the 6 mm cathode at the same capacitance. It is possible that this disparity exists for a similar reason to the current maxima with the larger diameter cathode. The data taken for the large cathode were taken in quick succession, warming up the electrolyte water enough to increase the resistance of the water. With less current to flow, the time constant would not be as long. At 1373 μF, for example, τ_1 is the same for both cathode sizes. During this

time, there is the most significant current flow. τ_2, however, is much smaller for 9 mm at 255 ± 54.6 ms than it is at 6 mm at 350 ± 47.4. Since most of the current has flowed through the system during τ_1, τ_2 is going to be faster since there is less remaining charge to dissipate.

4 Conclusions

In this work, a quantitative comparison of the effects of cathode size on the diagnostic characteristics of ball plasmoid discharges was presented. Although other groups studying ball plasmoids have used a broad range of cathode sizes and materials, none have presented a comparison of different cathode sizes and its impact on experimental variables. Observable properties (luminosity and lifetime) of ball plasmoids were analyzed, as well as electrical properties (current, voltage, and resistance). It can be concluded that changing the size of the cathode does not have any significant impact on the observable and electrical properties of ball plasmoid discharges to the extent we are able to detect. To gain a more complete understanding of this effect, it is reasonable to use a broader range of cathode sizes (and with different materials such as carbon, aluminum, or stainless steel) in order to examine if the same trends exist.

These results support and do not alter previous observations and analyses of ball plasmoid discharges. Specifically, increasing the size of the cathode used to produce plasmoids does not change trends in lifetime, luminosity, current and voltage dissipation, as well as the presence of two time constants which supports the existence of spark channels and a jet. In addition, spectroscopic analysis would be useful in determining if the cathode size has an effect on the emission of excited species in the plasmoid itself. The identity and quantity of excited species, as well as how they form and the reactions they induce will provide a better understanding of the reaction dynamics and even the lifetime of the plasmoid. Ultimately, understanding which variables have a significant effect on the various properties of plasmoids (i.e. input energy, cathode material, electrolyte composition, etc.) will help to isolate factors (i.e. number density of constituent species, vibrational excitation and subsequent reaction kinetics, etc.) that can help explain the extended lifetime and stability of ball plasmoids, and by extension, ball lightning.

References

[1] W. H. Bostick “Experimental Study of Ionized Matter Projected Across a Magnetic Field” *Phys. Rev.* (1956), **104**, 292-299.

[2] P. Xuexia, D. Zechao, J. Pengying, L. Weihua, L. Xia. “Influence of Ionization Degrees on the Evolutions of Charged Particles in Atmospheric Plasma at Low Altitude” *Plasma Sci. Technol.* (2012), **14**, 716.

[3] Y. Sakiyama, D. B. Graves, H. W. Chang, T. Shimizu, G. E. Morfill. “Plasma Chemistry Model of Surface Microdischarge in Humid Air and Dynamics of Reactive Neutral Species” *J. Phys. D: Appl. Phys.* (2012), **45**, 425201.

[4] A. Egorov, S. Stepanov. “Long-Lived Plasmoids Produced in Humid Air as Analogues of Ball Lightning” *Technical Physics.* (2002), **47**, 1584-1586.

[5] S. E. Dubowsky, A. N. Rose, N. Glumac, B. J. McCall. “The Electrical Properties and Physical Chemistry of Ball Plasmoid Discharges” *Plasma Sources Sci. Technol.* (2018) *Submitted.*

[6] D. M. Friday. “In Pursuit of a Chemical and Phenomenological Understanding of Long-Living Atmospheric Pressure Water-Based Ball Plasmoids” M.S. Thesis, University of Illinois Urbana-Champaign, 2014.

[7] J. Donoso, J. Trueba, A. Rañada. “The Riddle of Ball Lightning: A Review” *The Scientific World Journal* (2006), **6**, 254-278.

[8] W. N. Charman. “Ball Lightning” *Physics Reports.* (1979), **4**, 261-306.

[9] D. ter Haar. “An Electrostatic-Chemical Model of Ball Lightning” *Phys. Scr.* (1989), **39**, 735-740.

[10] J. Cen, P. Yuan, S. Xue. “Observation of the Optical and Spectral Characteristics of Ball Lightning” *Phys. Rev. Let.* (2014), **112**, 035001.

[11] J. Abrahamson. “Ball Lightning from Atmospheric Discharges via Metal Nanosphere Oxidation: from Soils, Wood or Metals” *Phil. Trans. R. Soc. Lond. A* (2002), **360**, 61-88.

[12] A. Guile. “Arc-Electrode Phenomena” *Proc. IEE, IEE Reviews* (1971), **118**, 1131-1154.

[13] V. Stelmashuk, P. Hoffer. “Experimental Study of a Long-Living Plasmid Using High-Speed Filming” *IEEE Transactions on Plasma Science* (2017), **45**, 3160-3165.

[14] K. D. Stephan, S. Dumas, L. Komala-Noor, J. McMinn. “Initiation, Growth, and Plasma Characteristics of ‘Gatchina’ Water Plasmoids” *Plasma Sources Sci. Thechnol.* (2013), **22**, 025018.

[15] A. Versteegh, K. Behringer, U. Fantz. G. Fussman, B. Jüttner, S. Noack. “Long-Living Plasmoids from Atmospheric Water Discharge” *Plasma Sources Sci. Thechnol.* (2008), **17**, 0204014.

[16] Y. Sakawa, K. Sugiyama, T. Tanabe, R. More. “Fireball Generation in a Water Discharge” *Plasma and Fusion Research: Rapid Communications* (2006), **1 (039)**, 1-2.

[17] N. Hayashi, H. Satomi, T. Mohri, T. Kajiwara, T. Tanabe. “General Nature of Luminous Body Transition Produced by Pulsed Discharge on an Electrolyte Solution in the Atmosphere” *IEEJ Transactions on Electrical and Electronic Engineering* (2009), **4**, 674-676.

[18] U. Fantz, S. Kalafat, R. Friedl, S. Briefi. “Generation of an Atmospheric Plasmoid from a Water Discharge: an Analysis of the Dissipated Energy” *J. Appl. Phys.* (2013), **114**, 1-8.

[19] S. E. Dubowsky, D. M. Friday, K. C. Peters, Z. Zhao, R. H. Perry, B. J. McCall. “Mass Spectrometry of Atmospheric-Pressure Ball Plasmoids” *International Journal of Mass Spectrometry* (2015), **376**, 39-45.

[20] D. M. Friday, P. B. Broughton, T. A. Lee, G. A Schutz, J. N. Betz, C. M. Lindsay. “Further Insight into the Nature of Ball-Lightning-Like Atmospheric Pressure Plasmoids” *J. Phys. Chem. A* (2013), **117**, 9931-9940.